2. Theoretical and Experimental Studies of the Total Emittance of Metals

W. J. PARKER AND G. L. ABBOTT

U.S. NAVAL RADIOLOGICAL DEFENSE LABORATORY, SAN FRANCISCO, CALIF.

Equations are presented for the spectral emissivity of metals as a function of angle and plane of polarization based on the Drude free-electron model taking electronic relaxation into account. These equations are integrated to obtain more general expressions than now exist for the total normal and total hemispherical emissivity of metals. Total emittance measurements have been made on tungsten, tantalum, niobium, and molybdenum. These are compared with the theoretical emissivity equations, and a qualitative, but not a quantitative, agreement is found between them. It is necessary to take other factors into account in order to explain the observed emittance data.

There are two theoretical equations developed by Foote (ref. 1) and by Davisson and Weeks (ref. 2) which relate the total normal and the total hemispherical emittance of metals to their electrical resistivity. In the derivation of these equations, it was assumed that the mean free time between collisions of the electron and the lattice is small compared with the period of the electromagnetic wave. This assumption is not completely valid for metals throughout most of the wavelength region in which they emit thermal radiation. In this article a general expression for the spectral emissivity is written down and integrated over all wavelengths and angles to obtain equations for the total normal and the total hemispherical emittance which take the relaxation time of the electron into account.

The total hemispherical emittance and the total normal emittance were measured on clean specular surfaces of tungsten, tantalum, niobium, and molybdenum over a temperature range of 1000° to 3000° K (depending on the material); and the electrical resistivities of the metals were also measured over the same temperature range. The total hemispherical emittance was obtained from the measured power dissipation within the uniform temperature region of an electrically heated ribbon specimen. The temperature was measured with tungsten/tungsten, 26-percent rhenium thermocouples which had been specially calibrated. The total normal emittance was determined with a radiation thermopile. The ratio of total hemispherical emittance to total normal emittance was also calculated directly from the angular distribution obtained by rotating the ribbon within the field of view of the thermopile. The data so obtained have been compared with the results predicted by the theoretical equations referred to above.

Direct measurements of the normal spectral emittance out to 5 μ are now being made on the refractory metals by using three metal ribbons to form a closed tube of triangular cross section. The radiation from a small rectangular hole in one of the ribbons is compared with the radiation from the surface adjacent to it with a Perkin-Elmer double-pass monochrometer as in the method used by De Vos (ref. 3). These measurements will be made for wavelengths up to 25 μ as a function of angle for

both planes of polarization. The spectral emittance data will be compared with the results predicted by the theoretical spectral emissivity equations. The data will also be integrated with respect to wavelength to determine the total emittance, which can then be compared with the total emittance values already measured directly.

The study of emissivity can provide additional insight into the microscopic phenomena occurring in solids, particularly near their surfaces. While the spectral emissivity is capable of providing a more detailed picture, the total emittance, particularly the total hemispherical emittance, in many cases can be determined much more readily and more accurately. Any complete theory of emissivity must be able to predict the total emissivity and its variation with temperature. Furthermore, from an engineering point of view it is the total hemispherical emittance which is usually of primary concern in matters that involve radiant heat transfer.

SYMBOLS

a	Relaxation parameter, $1.31\times 10^{11}\tau T=y/x$
C_1	Planck's first radiation constant
C_2	Planck's second radiation constant
c	Velocity of light
D	Complex dielectric constant
D'	Real part of dielectric constant
D''	Imaginary part of dielectric constant
e	Electronic charge
i	$\sqrt{-1}$
J	Spectral intensity given by the Planck distribution, radiant power per unit area per unit wavelength interval
j	$[(1+y^2)^{1/2}-y]^{1/2}$
m	Mass of the electron
N	Number of free electrons per unit volume
T	Absolute temperature
x	$C_2/\lambda T$
y	$\omega\tau$
Z_n	Defined by the equation $\epsilon_n=2/(1+Z_n)$
Z_p	Defined by the equation $\epsilon_p=2/(1+Z_p)$
ϵ_H	Total hemispherical emissivity
ϵ_λ	Spectral hemispherical emissivity (including both planes of polarization)
ϵ_N	Total normal emissivity
ϵ_n	Spectral emissivity (electric vector normal to the plane of emergence); ϵ_n is a function of θ
$\epsilon_{n\lambda}$	Spectral hemispherical emissivity (electric vector normal to the plane of emergence)
ϵ_o	Normal spectral emissivity (including both planes of polarization)
ϵ_p	Spectral emissivity (electric vector in the plane of emergence); ϵ_p is a function of θ
$\epsilon_{p\lambda}$	Spectral hemispherical emissivity (electric vector parallel to the plane of emergence)
θ	Angle of incidence or emergence of radiation
λ	Wavelength
ρ	Electrical resistivity
σ	Stefan-Boltzmann constant
τ	Electronic relaxation time
ω	Angular frequency of the electromagnetic wave

BACKGROUND

The thermal radiation from a solid surface can best be described in terms of its absolute temperature and its emittance. If the surface is black, that is, if it absorbs all of the energy impinging upon it, it will radiate in accordance with the following laws of blackbody radiation.

(1) Stefan-Boltzmann law: The total radiant power emitted per unit area is given by $H=\sigma T^4$ where σ is the Stefan-Boltzmann constant and T is the absolute temperature.

(2) Planck's law: The spectral distribution of the radiation in radiant power per unit area per unit wavelength interval is given by

$$J=C_1\lambda^{-5}[\exp(C_2/\lambda T)-1]^{-1}$$

where C_1 and C_2 are Planck's first and second radiation constants and λ is the wavelength.

(3) Lambert's cosine law: The intensity of the radiation is proportional to the cosine of the angle of emergence. From this law it follows that the total normal and the spectral normal intensities in units of radiant power per unit area per steradian and radiant power per unit area per unit wavelength interval per steradian are equal to H/π and J/π, respectively.

(4) The intensity of the radiation at any angle is independent of the plane of polarization.

Emittance is the property of a real surface; it is the ratio of the rate of emission of radiant energy from the surface to the rate of emission from a blackbody radiator at the same temperature under the same conditions. Emissivity is a fundamental property of a material and is numerically equal to the emittance of a specimen of the material that has an optically smooth surface and is sufficiently thick to be opaque. It is further assumed that the surface is

free from contamination and that the crystalline structure, and its defects adjacent to the surface are the same as those of the interior. The emittance and emissivity can be either normal, angular, or hemispherical, depending upon whether the comparison with the black surface is of the intensity radiated normal to the surface, of that emitted at some other angle, or of the power radiated over all angles. They can also be either spectral or total, depending upon whether the comparison is made with monochromatic radiation or whether it includes the radiation at all wavelengths. These parameters will in general be different for each plane of polarization, except for normal emergence.

General expressions will be developed in this article which relate the spectral emissivity to the complex dielectric constant. These equations will be written down specifically for metals, making use of the complex dielectric constant which takes the electronic relaxation time into account. An equation for the total normal emissivity will be obtained by integrating the intensity at normal emergence over all wavelengths and dividing it by the normal blackbody intensity. An expression for the total hemispherical emissivity will be found by integrating over all angles for each plane of polarization as well as over the entire wavelength range.

SPECTRAL EMISSIVITY

Consider, first, a homogeneous and opaque solid at a uniform temperature T with a perfectly specular surface. Blackbody conditions exist in the interior of the solid and blackbody radiation impinges on its inner surface. A fraction R of this radiation is internally reflected and a fraction $\epsilon=1-R$ escapes, where ϵ is the emissivity.

In texts on optics or electromagnetic theory (ref. 4) the reflectivities are given by

$$R_n=\frac{\sin^2(\theta-\phi)}{\sin^2(\theta+\phi)}$$

and

$$R_p=\frac{\tan^2(\theta-\phi)}{\tan^2(\theta+\phi)}$$

where R_n is the reflectivity for radiation whose electric vector is normal to the plane of incidence, R_p is the reflectivity for radiation whose electric vector lies in the plane of incidence, θ is the angle of incidence, and ϕ is the angle of refraction. According to Snell's law, $\sin\theta=n\sin\phi$, where n is the index of refraction, which is equal to the square root of the dielectric constant D for insulators. The reflectivities in terms of the angle of incidence are given by

$$R_n=\left|\frac{\cos\theta-(D-\sin^2\theta)^{1/2}}{\cos\theta+(D-\sin^2\theta)^{1/2}}\right|^2 \tag{1}$$

and

$$R_p=\left|\frac{D\cos\theta-(D-\sin^2\theta)^{1/2}}{D\cos\theta+(D-\sin^2\theta)^{1/2}}\right|^2 \tag{2}$$

These expressions are satisfactory for an absorbing medium if the dielectric constant is considered to be complex so that $D=D'+iD''$.

Since $\epsilon=1-R$, some algebraic manipulation of equations (1) and (2) leads to the following expressions for the emissivity for radiation polarized normal and parallel respectively to the plane of emergence:

$$\epsilon_n=\frac{2}{1+Z_n}\qquad \epsilon_p=\frac{2}{1+Z_p} \tag{3}$$

where Z_n and Z_p are given by

$$Z_n=\frac{[(D'-\sin^2\theta)^2+D''^2]^{1/2}+\cos^2\theta}{\sqrt{2}\cos\theta[((D'-\sin^2\theta)^2+D''^2)^{1/2}+D'-\sin^2\theta]^{1/2}} \tag{4}$$

$$Z_p=\frac{[(D'-\sin^2\theta)^2+D''^2]^{1/2}+(D'^2+D''^2)\cos^2\theta}{\left[\begin{array}{r}\sqrt{2}\cos\theta[((D'-\sin^2\theta)^2+D''^2)^{1/2}(D'^2\\ +D''^2)+(D'^2-\sin^2\theta)(D'^2-D''^2)\\ +2D'D''^2]^{1/2}\end{array}\right]} \tag{5}$$

In this article the classical contribution of the free electrons to the emissivity of metals is considered. The effect of the bound electrons, the internal photoelectric effect, and the anomalous skin effect will not be treated. The spectral emissivity equations taking the electronic relaxation time of the free electrons into account are developed here.

From Mott and Jones (ref. 5) the dielectric constant of a metal, considering only the free

electrons, is given by

$$D=1-\frac{4\pi Ne^2\tau^2}{m(\omega^2\tau^2+1)}-i\,\frac{4\pi Ne^2\tau/\omega}{m(\omega^2\tau^2+1)}$$

since $D=n^2-k^2+2\,ink$, where n is the index of refraction and k is the index of absorption. N is the number of free electrons per unit volume, e is the electronic charge in statcoulombs, τ is the relaxation time, m is the mass of the electron, and ω is the angular frequency. This can be written

$$D=1-\frac{y+i}{1+y^2}\,\frac{4\pi Ne^2}{m}\,\frac{\tau}{\omega} \tag{6}$$

where $y=\omega\tau$. Since the electrical resistivity ρ (in statohm-centimeters), is equal to

$$\rho=\frac{m}{Ne^2\tau} \tag{7}$$

and $\omega=(2\pi c)/\lambda$ where λ is the wavelength and c is the velocity of light, then $D=1-[(y+i)/(1+y^2)](2/c)(\lambda/\rho)$. If λ is expressed in centimeters, and ρ in ohm-centimeters, then in

$$D=1-\frac{y+i}{1+y^2}\,\frac{60\lambda}{\rho} \tag{8}$$

where D is dimensionless, the constant 60 having units of ohms^{-1}. From the preceding equations

$$y=\omega\tau=\frac{2\pi cm}{\lambda\rho Ne^2}=1.1\times10^{-9}V/S\rho\lambda \tag{9}$$

where V is the atomic volume, S is the effective number of free electrons per atom, and again ρ and λ are in ohm-centimeters and centimeters.

In order that the first term, 1, on the right-hand side of equation (8) and the term $\sin^2\theta$ in equations (4) and (5) be negligible, either $[1/(1+y^2)](60\lambda/\rho)>>1$, or $[y/(1+y^2)](60\lambda/\rho)>>1$. About 99 percent of the thermal radiation from a black surface occurs for λT greater than 0.13, so the inequality

$$\rho T<<\frac{7.8}{1+y^2}\text{ or }\rho T<<\frac{7.8y}{1+y^2} \tag{10}$$

is a necessary condition if equation (8) is to hold. When y is small the first inequality holds adequately well for all of the metals. When y is large, the second inequality becomes $\rho T<<7.8/y$. Usually V/S is about 10 so that $1/y\approx10^8\rho\lambda$ and the second inequality simplifies to $T<<10{,}000°$ K. This temperature is based on the short-wavelength limit at $\lambda T=0.13$. At λT for the maximum of the spectral distribution $T<<15{,}000°$ K. If these approximations are assumed to hold, $y=D'/D''$ and equations (4) and (5) can be rewritten as

$$Z_n=\frac{(1+y^2)^{1/4}}{\sqrt{2}j}\left[\left(\frac{\rho}{60\lambda}\right)^{1/2}\frac{(1+y^2)^{1/4}}{(\cos\theta)^{-1}}+\left(\frac{60\lambda}{\rho}\right)^{1/2}\frac{(\cos\theta)^{-1}}{(1+y^2)^{1/4}}\right] \tag{11}$$

$$Z_p=\frac{(1+y^2)^{1/4}}{\sqrt{2}j}\left[\left(\frac{\rho}{60\lambda}\right)^{1/2}\frac{(1+y^2)^{1/4}}{\cos\theta}+\left(\frac{60\lambda}{\rho}\right)^{1/2}\frac{\cos\theta}{(1+y^2)^{1/4}}\right] \tag{12}$$

where

$$j=[(1+y^2)^{1/2}-y]^{1/2}\text{ so that }1/j=[(1+y^2)^{1/2}+y]^{1/2}. \tag{13}$$

Since

$$\left(\frac{\rho}{60\lambda}\right)^{1/2}(1+y^2)^{1/4}<<\left(\frac{60\lambda}{\rho}\right)^{1/2}\frac{1}{(1+y^2)^{1/4}}$$

except for very large values of y, which are not of concern here, the normal-emergence value of Z, which is the same for both planes of polarization, is given by

$$Z_n=Z_p=\left(\frac{30\lambda}{\rho}\right)^{1/2}[(1+y^2)^{1/2}-y]^{-1/2} \tag{14}$$

and the normal spectral emissivity is given by

$$\epsilon_0=\frac{2}{\frac{1}{j}\left(\frac{30\lambda}{\rho}\right)^{1/2}+1}=2\sum_{m=1}^{\infty}(-1)^{m+1}j^m\left(\frac{\rho}{30\lambda}\right)^{m/2}. \tag{15}$$

TOTAL EMISSIVITY

The spectral distribution of intensity normal to the surface of a perfectly black radiator in radiant power per unit area per unit wavelength interval per steradian is given by

$$\frac{J}{\pi}=\frac{C_1}{\pi}\frac{1}{\lambda^5}\left[\exp\left(\frac{C_2}{\lambda T}\right)-1\right]^{-1}. \quad (16)$$

Integrating equation (16) over all wavelengths gives the radiant power per unit area per steradian:

$$\int_0^\infty \frac{J}{\pi}\,d\lambda=\frac{C_1}{\pi}\int_0^\infty \frac{1}{\lambda^5}\left[\exp\left(\frac{C_2}{\lambda T}\right)-1\right]^{-1}d\lambda=\frac{\sigma T^4}{\pi} \quad (17)$$

where $\sigma=(C_1/15)(\pi/C_2)^4$ is the Stefan-Boltzmann constant.

In order to determine the total normal emissivity it is necessary to multiply the spectral emissivity, equation (15), by the normal Planck distribution, equation (16), integrate over all wavelengths, and divide by $\sigma T^4/\pi$. That is,

$$\epsilon_N=\frac{\pi}{\sigma T^4}\int_0^\infty \frac{\epsilon_0 J\,d\lambda}{\pi}$$

$$=\frac{30C_2^4}{\pi^4T^4}\sum_{m=1}^{\infty}\sum_{n=1}^{\infty}\int_0^\infty (-1)^{m+1}j^m \left(\frac{\rho}{30\lambda}\right)^{m/2}\frac{1}{\lambda^5}\exp\left(\frac{-nC_2}{\lambda T}\right)d\lambda$$

By letting $x=C_2/T$

$$\epsilon_N=\frac{30}{\pi^4}\sum_{m=1}^{\infty}\sum_{n=1}^{\infty}\int_0^\infty (-1)^{m+1}j^m \left(\frac{\rho T}{30C_2}\right)^{m/2}x^{3+(m/2)}\exp(-nx)dx \quad (18)$$

It is useful first to consider the case where the electronic relaxation time can be neglected. In this case $j=1$, and equation (18) becomes

$$\epsilon_N=\frac{30}{\pi^4}\sum_{m=1}^{\infty}(-1)^{m+1}\left(\frac{\rho T}{30C_2}\right)^{m/2}\sum_{n=1}^{\infty}\int_0^\infty x^{3+(m/2)}\exp(-nx)dx \quad (19)$$

$$=\frac{30}{\pi^4}\sum_{m=1}^{\infty}(-1)^{m+1}\left(\frac{\rho T}{30C_2}\right)^{m/2}\sum_{n=1}^{\infty}\frac{\Gamma\left(4+\frac{m}{2}\right)}{n^{4+(m/2)}} \quad (20)$$

$$=0.578(\rho T)^{1/2}-0.178(\rho T)+0.0584(\rho T)^{3/2}-\ldots \quad (21)$$

This result is identical with that of Foote except that it takes into account one more term which is needed at larger values of ρT. The coefficient of the third term for the total normal emissivity was erroneously given as 0.044 in the article by Davisson and Weeks (ref. 2).

As it is given in equation (13), j and its second and third powers make equation (18) unwieldy to integrate. Therefore, the following approximations to j, j^2, and j^3, designated as j_*, j_*^2, and j_*^3, respectively, were used to simplify the integration.

$$j_*=0.430\exp(-1.05y)+0.330\exp(-0.245y)+0.240\exp(-0.0207y) \quad (22)$$

$$j_*^2=0.700\exp(-1.32y)+0.240\exp(-0.31y)+0.060\exp(-0.043y) \quad (23)$$

$$j_*^3=0.560\exp(-2.43y)+0.400\exp(-0.79y)+0.040\exp(-0.125y) \quad (24)$$

The accuracy with which these three expressions approximate j, j^2, and j^3 over the significant range of y is demonstrated in table I.

From equation (9)

$$y=\omega\tau=\frac{2\pi c}{C_2}\tau T x=ax$$

where $a=1.31\times10^{11}\tau T$ and $x=C_2/\lambda T$. The product τT is independent of wavelength and only mildly variant with temperature for the metals. This quantity, derived by using equation (7), is tabulated in table II. The values listed in this table are bulk properties and may be different at the surface where the radiating properties are controlled.

When $j\neq1$, the first three terms for the total normal emissivity are then given as:

$$\epsilon_N=\frac{30}{\pi^4}\left(\frac{\rho T}{30C_2}\right)^{1/2}\sum_{n=1}^{\infty}\int_0^\infty x^{3.5}\{0.43\exp[-(n+1.05a)x]+0.33\exp[-(n+0.245a)x]+0.24\exp[-(n+0.0207a)x]\}dx$$

$$+\frac{30}{\pi^4}\left(\frac{\rho T}{30C_2}\right)\sum_{n=1}^{\infty}\int_0^\infty x^4\{0.70\exp[-(n+1.32a)x]+0.24\exp[-(n+0.31a)x]$$

TABLE I.—*Comparison of* j, j_1, j_2, *and* j_3 *with Approximate Values Given by Equations (22), (23), and (24)*

y	j	j_a	Error, percent	j^2	j_a^2	Error, percent	j^3	j_a^3	Error, percent
0	1	1	0	1	1	0	1	1	0
0.1	0.950	0.949	0.11	0.903	0.907	0.44	0.858	0.857	0.12
.2	.905	.905	0	.820	.823	.37	.742	.728	1.89
.4	.822	.819	.37	.677	.684	1.03	.556	.542	2.52
.6	.751	.751	0	.565	.574	1.59	.425	.417	1.88
.8	.692	.693	.14	.480	.488	1.67	.333	.330	.90
1.0	.642	.642	0	.413	.421	1.93	.265	.266	.38
1.2	.600	.602	.33	.360	.367	1.94	.216	.219	1.39
1.4	.565	.566	.18	.320	.320	0	.181	.184	1.65
1.6	.535	.535	0	.286	.287	.35	.153	.158	3.27
1.8	.510	.508	.39	.260	.259	.38	.133	.135	1.50
2.0	.486	.485	.21	.236	.234	.85	.115	.117	1.74
4.0	.351	.351	0	.123	.119	3.25	.0431	.0420	2.55
6.0	.288	.288	0	.083	.083	0	.0239	.023	.42
8.0	.249	.249	0	.062	.063	1.61	.0154	.0155	.65
10.0	.223	.224	.45	.0499	.050	.20	.0111	.0115	3.60
15.0	.182	.184	1.10	.0333	.033	.90	.0061	.0061	0
20.0	.158	.160	1.27	.025	.025	0	.0039	.0033	15.4
25.0	.141	.143	1.42	.020	.0205	2.5	.0028	.0018	37.7
30.0	.129	.129	0	.0167	.0166	.60	.0022	.0010	54.6

$$+0.06\exp[-(n+0.043a)x]\}dx$$

$$+\frac{30}{\pi^4}\left(\frac{\rho T}{30C_2}\right)^{3/2}\sum_{n=1}^{\infty}\int_0^{\infty}x^{4.5}\{0.56\exp[-(n+2.43a)x]+0.40\exp[-(n+0.79a)x]+0.04\exp[-(n+0.125a)x]\}dx. \quad (25)$$

The integrals appearing in equation (25) and their solutions are of the form

$$\int_0^{\infty}x^z\exp[-(n+k)x]dx=\frac{\Gamma(z+1)}{(n+k)^{z+1}}.$$

The quantity

$$\sum_{n=1}^{\infty}\left(\frac{1}{n+k}\right)^{z+1}\div\sum_{n=1}^{\infty}\left(\frac{1}{n}\right)^{z+1}\equiv q_z$$

can be approximated for $z=3.5$, 4.0, and 4.5 by the functions

$$q'_{3.5}=(1+k)^{-4.33},\ q'_{4.0}=(1+k)^{-4.85},$$

and $q'_{4.5}=(1+k)^{-5.38}$.

The accuracy of this approximation is demonstrated in table III.

These relationships can be used to evaluate equation (25) in terms of the emissivity in the $y=0$ case. Hence

$$\epsilon_N=\left[\frac{0.430}{(1+1.05a)^{4.33}}+\frac{0.330}{(1+0.245a)^{4.33}}+\frac{0.240}{(1+0.0207a)^{4.33}}\right]0.578(\rho T)^{1/2}$$

$$-\left[\frac{0.700}{(1+1.32a)^{4.85}}+\frac{0.240}{(1+0.31a)^{4.85}}+\frac{0.0600}{(1+0.043a)^{4.85}}\right]0.178(\rho T)$$

$$+\left[\frac{0.560}{(1+2.43a)^{5.38}}+\frac{0.400}{(1+0.79a)^{5.38}}+\frac{0.0400}{(1+0.125a)^{5.38}}\right]0.0584(\rho T)^{3/2} \quad (26)$$

which can be written

$$\epsilon_N=0.578p_1(\rho T)^{1/2}-0.178p_2(\rho T)+0.0584p_3(\rho T)^{3/2} \quad (27)$$

TABLE II.—*Relaxation Times and Electrical Resistivities at Room Temperature.*

Metal	τ, sec (10^{-14})*	τT, deg-sec (10^{-12})*	a	ρ, ohm-cm	$(\rho/T)^{1/2}$, $(\text{ohm-cm/deg})^{1/2}$ (10^{-4})*
Lithium	8. 6	2. 3	0. 30	9. 2	1. 77
Sodium	31	8. 5	1. 1	4. 7	1. 27
Potassium	44	12	1. 6	6. 6	1. 5
Rubidium	27	7. 4	. 97	12. 5	2. 07
Cesium	21	5. 7	. 75	19. 9	2. 61
Copper	27	7. 3	. 96	1. 72	. 77
Silver	41	11	1. 5	1. 59	. 74
Gold	29	7. 9	1. 0	2. 44	. 91
Nickel	9. 8	2. 7	. 35	7. 8	1. 63
Cobalt	9. 2	2. 5	. 33	9. 8	3. 34
Iron	24	6. 6	. 87	10. 0	1. 85
Palladium	9. 2	2. 5	. 33	11. 0	1. 94
Platinum	9. 0	2. 5	. 32	10. 0	1. 85

*Multiply each value in column by this factor.

where the multiplier function p is tabulated in table IV and plotted as a function of a in figure 1. Values of a for several of the metals are listed in table II.

Equation (27) can now be written explicitly for the values of a used in table IV which includes essentially the whole range of a values encountered in metals. For

$$a=0 \quad \epsilon_N=0.578(\rho T)^{1/2}-0.178(\rho T)+0.0584(\rho T)^{3/2}$$

$$a=0.2 \quad \epsilon_N=0.403(\rho T)^{1/2}-0.0826(\rho T)+0.0165(\rho T)^{3/2}$$

$$a=0.5 \quad \epsilon_N=0.290(\rho T)^{1/2}-0.0417(\rho T)+0.00606(\rho T)^{3/2}$$

$$a=1.0 \quad \epsilon_N=0.212(\rho T)^{1/2}-0.0219(\rho T)+0.00234(\rho T)^{3/2}$$

$$a=1.5 \quad \epsilon_N=0.175(\rho T)^{1/2}-0.0153(\rho T)+0.00128(\rho T)^{3/2} \qquad (28)$$

These equations are shown graphically in figure 2. The factor $(\rho T)^{1/2}$ is conveniently written as $(\rho/T)^{1/2}T$, where $(\rho/T)^{1/2}$ is only a mild function of temperature and is listed for several of the metals in table II.

In order to get the total hemispherical emissivity we must go back to the equations of spectral emissivity as a function of angle and plane of polarization. From equations (11) and (12) we can write:

$$Z_n=A\left(\frac{B}{\cos\theta}+\frac{\cos\theta}{B}\right)$$

TABLE III.—*Comparison of Approximate Functions*

k	$q_{2.5}$	$q'_{2.5}$	$q_{4.0}$	$q'_{4.0}$	$q_{4.5}$	$q'_{4.5}$
0. 02	0. 915	0. 918	0. 907	0. 908	0. 898	0. 899
. 05	. 805	. 810	. 787	. 789	. 767	. 769
. 10	. 659	. 662	. 627	. 629	. 598	. 598
. 20	. 452	. 454	. 411	. 412	. 374	. 374
. 50	. 173	. 173	. 140	. 140	. 113	. 113
1. 00	. 051	. 050	. 036	. 035	. 025	. 024
2. 00	. 009	. 009	. 005	. 005	. 003	. 003

TABLE IV.—*Values of the Multiplier Functions* p_1, p_2, *and* p_3 *for a Range of Values of the Relaxation Parameter* a

a	p_1	$1p_2$	p_3
0. 0	1. 000	1. 000	1. 000
. 2	. 697	. 464	. 283
. 5	. 501	. 234	. 104
1. 0	. 367	. 123	. 040
1. 5	. 303	. 086	. 022

$$Z_p = A\left(B\cos\theta + \frac{1}{B\cos\theta}\right)$$

where

$$A = (2)^{-1/2}[1-(1+1/y^2)^{-1/2}]^{-1/2} = \frac{(1+y^2)^{1/4}}{\sqrt{2}j}$$

and

$$B = \left(\frac{60\lambda}{\rho}\right)^{1/2}\frac{1}{(1+y^2)^{1/4}}$$

Hence, from equations (3)

$$\epsilon_n = \frac{2B\cos\theta}{B\cos\theta + AB^2 + A\cos^2\theta} \tag{29}$$

$$\epsilon_p = \frac{2B\cos\theta}{B\cos\theta + AB^2\cos^2\theta + A} \tag{30}$$

In all cases $B^2 >> \cos\theta$, so that ϵ_n reduces to

$$\epsilon_n = \frac{2B\cos\theta}{B\cos\theta + AB^2} \tag{31}$$

The spectral hemispherical emissivity is defined by

$$\epsilon_h J \equiv \int_0^{\pi/2} (\epsilon_n + \epsilon_p)\frac{J}{2\pi}\cos\theta\, 2\pi\sin\theta\, d\theta \tag{32}$$

A fraction $1/(2\pi)$ of the radiation from a blackbody appears in a unit solid angle normal to the surface for each plane of polarization. The energy radiated per unit solid angle is proportional to the cosine of the angle for each plane of polarization for radiation from a black surface. Considering each plane separately,

$$\epsilon_h = \frac{\epsilon_{nh}}{2} + \frac{\epsilon_{ph}}{2}$$

where

$$\frac{\epsilon_{nh}}{4B} = \int_0^1 \frac{\cos^2\theta\, d\cos\theta}{B\cos\theta + AB^2} \tag{33}$$

$$\frac{\epsilon_{ph}}{4B} = \int_0^1 \frac{\cos^2\theta\, d\cos\theta}{B\cos\theta + AB^2\cos^2\theta + A} \tag{34}$$

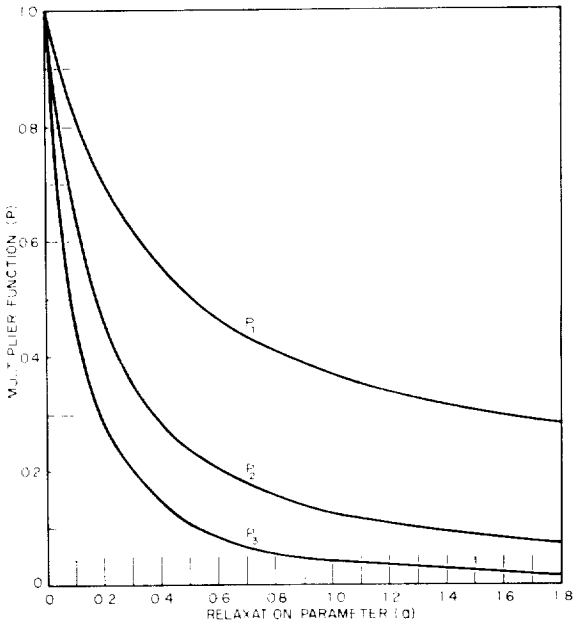

FIGURE 1.—*Multiplier functions.*

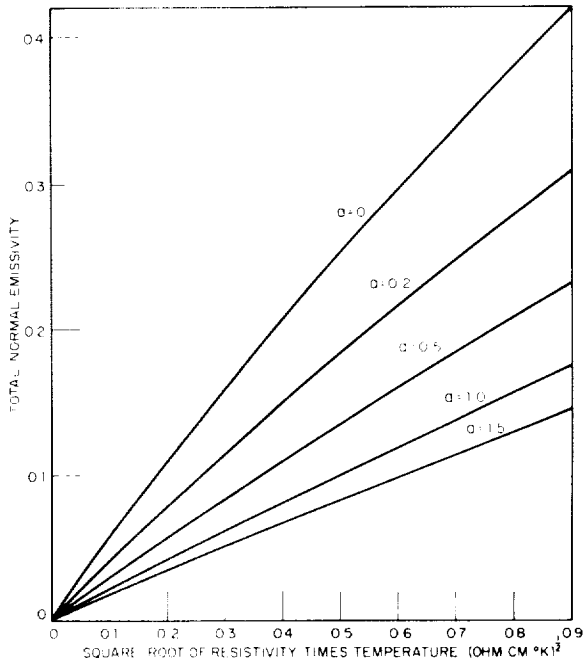

FIGURE 2.—*Total normal emissivity.*

The integration of equation (33) leads to

$$\frac{\epsilon_{nh}}{4}=\frac{1}{2}-AB+(AB)^2\log\left(1+\frac{1}{AB}\right)$$

If the logarithm is expanded,

$$\frac{\epsilon_{nh}}{4}=\frac{1}{3}\frac{1}{AB}-\frac{1}{4}\left(\frac{1}{AB}\right)^2+\frac{1}{5}\left(\frac{1}{AB}\right)^3+\cdots$$

which is equal to

$$\frac{\epsilon_{nh}}{4}=\frac{j}{3}\left(\frac{\rho}{30\lambda}\right)^{1/2}-\frac{j^2}{4}\left(\frac{\rho}{30\lambda}\right)+\frac{j^3}{5}\left(\frac{\rho}{30\lambda}\right)^{3/2}+\cdots. \tag{35}$$

The integration of equation (34) yields

$$\frac{\epsilon_{ph}}{4}=\frac{1}{AB}-\left(\frac{1}{AB}\right)^2\left\{\log B-\frac{1-2A^2}{(4A^2-1)^{1/2}}\left[\tan^{-1}\frac{2AB+1}{(4A^2-1)^{1/2}}-\tan^{-1}\frac{1}{(4A^2-1)^{1/2}}\right]\right\}-\frac{1}{2}\left(\frac{1}{AB}\right)^3$$

which is equal to

$$\frac{\epsilon_{ph}}{4}=j\left(\frac{\rho}{30\lambda}\right)^{1/2}-j^2\left(\frac{\rho}{30\lambda}\right)\left\{\log\left[\left(\frac{60\lambda}{\rho}\right)^{1/2}(1+y^2)^{-1/4}\right]+y\left\{\tan^{-1}\left[\left(\frac{30\lambda}{\rho}\right)^{1/2}2j+j^2\right]-\tan^{-1}j^2\right\}\right\}-\frac{j^3}{2}\left(\frac{\rho}{30\lambda}\right)^{3/2}+\cdots. \tag{36}$$

Before proceeding further, the equation for the total hemispherical emissivity, ϵ_H, will be derived on the assumption that the electronic relaxation time is negligibly small. In this case $y=0$ and $j=1$ so that

$$\frac{\epsilon_{nh}}{4}=\frac{1}{3}\left(\frac{\rho}{30\lambda}\right)^{1/2}-\frac{1}{4}\left(\frac{\rho}{30\lambda}\right)+\frac{1}{5}\left(\frac{\rho}{30\lambda}\right)^{3/2}-\cdots \tag{37}$$

$$\frac{\epsilon_{ph}}{4}=\left(\frac{\rho}{30\lambda}\right)^{1/2}-\frac{1}{2}\left(\frac{\rho}{30\lambda}\right)\log\left(\frac{60\lambda}{\rho}\right)-\frac{1}{2}\left(\frac{\rho}{30\lambda}\right)^{3/2}+\cdots \tag{38}$$

$$\epsilon_h=\frac{\epsilon_{nh}}{2}+\frac{\epsilon_{ph}}{2}=\frac{8}{3}\left(\frac{\rho}{30\lambda}\right)^{1/2}-\left(\frac{1}{2}+\log\frac{60\lambda}{\rho}\right)\left(\frac{\rho}{30\lambda}\right)-\frac{3}{5}\left(\frac{\rho}{30\lambda}\right)^{3/2}+\cdots. \tag{39}$$

The spectral hemispherical emissivity must be multiplied by the Planck distribution, integrated over all wavelengths, and divided by the total radiation from a blackbody to determine the total hemispherical emissivity. Thus,

$$\epsilon_H=\int_0^\infty\frac{\epsilon_h J\,d\lambda}{\sigma T^4}=\frac{1}{\sigma T^4}\int_0^\infty\epsilon_h\frac{C_1}{\lambda^5}\sum_1^\infty\exp\left(-\frac{nC_2}{\lambda T}\right)d\lambda. \tag{40}$$

By the previous substitution $x=C_2/\lambda T$,

$$\epsilon_h=\frac{8}{3}\left(\frac{\rho T}{30C_2}\right)^{1/2}x^{1/2}-\left(\frac{1}{2}+\log\frac{60C_2}{\rho T}-\log x\right)\frac{\rho Tx}{30C_2}-\frac{3}{5}\left(\frac{\rho T}{30C_2}\right)^{3/2}x^{3/2}$$

or simply

$$\epsilon_h=A_Hx^{1/2}-B_Hx+C_Hx\log x-D_Hx^{3/2}$$

where

$$A_H=\frac{8}{3}\left(\frac{\rho T}{30C_2}\right)^{1/2}\qquad B_H=\left(\frac{1}{2}+\log\frac{60C_2}{\rho T}\right)$$

$$C_H=\left(\frac{\rho T}{30C_2}\right)\qquad D_H=\frac{3}{5}\left(\frac{\rho T}{30C_2}\right)^{3/2}$$

and

$$\epsilon_H=\frac{C_1}{\sigma C_2^4}\int_0^\infty(A_Hx^{1/2}-B_Hx+C_Hx\log x-D_Hx^{3/2})x^3\sum_{n=1}^\infty\exp(-nx)dx$$

Since

$$\sigma=\frac{\pi^4}{15}\frac{C_1}{C_2^4}$$

$$\frac{\pi^4}{15}\epsilon_H=A_H\int_0^\infty x^{3.5}\sum_{n=1}^\infty\exp(-nx)dx-B_H\int_0^\infty x^4\sum_{n=1}^\infty\exp(-nx)dx$$

$$+C_H\int_0^\infty x^4 \log x \sum_{n=1}^{\infty} \exp(-nx)\,dx$$

$$-D_H\int_0^\infty x^{4.5} \sum_{n=1}^{\infty} \exp(-nx)\,dx$$

$$\frac{\pi^4}{15}\epsilon_H = A_H\mathrm{I} - B_H\mathrm{II} + C_H\mathrm{III} - D_H\mathrm{IV}$$

The solutions of I, II, and IV are

$$\mathrm{I} = \sum_{n=1}^{\infty} \frac{\Gamma(4.5)}{n^{4.5}} = 12.264$$

$$\mathrm{II} = \sum_{n=1}^{\infty} \frac{4!}{n^5} = 24.885$$

$$\mathrm{IV} = \sum_{n=1}^{\infty} \frac{\Gamma(5.5)}{n^{5.5}} = 53.649$$

If $Z=nx$,

$$\mathrm{III} = \sum_{n=1}^{\infty} \int_0^\infty x^4 \log x \exp(-nx)\,dx$$

$$= \sum_{n=1}^{\infty} \frac{1}{n^5}\left[\int_0^\infty Z^4 \log Z \exp(-Z)\,dZ - \log n \int_0^\infty Z^4 \exp(-Z)\,dZ\right]$$

Integrating by parts gives

$$\int_0^\infty Z^4 \log Z \exp(-Z)\,dZ$$

$$= \int_0^\infty \log Z\, d\int Z^4 \exp(-Z)\,dZ$$

$$= \log Z \int Z^4 \exp(-Z)\,dZ\,\Big|_0^\infty - \int_0^\infty \frac{1}{Z}\int Z^4 \exp(-Z)\,dZ\,dZ$$

$$= -\log Z \exp(-Z)(Z^4+4Z^3+12Z^2+24Z+24)\Big|_0^\infty + \int_0^\infty \exp(-Z)\left(Z^3+4Z^2+12Z+24+\frac{24}{Z}\right)dZ = -24 \log Z \exp(-Z)\Big|_0^\infty + (3!) + 4(2!) + 12(1!) + 24 + 24\int_0^\infty \frac{1}{Z}\exp(-Z)\,dZ$$

$$= -24 \log Z \exp(-Z)\Big|_0^\infty + 50 + 24 \log Z \exp(-Z)\Big|_0^\infty + 24\int_0^\infty \log Z \exp(-Z)\,dZ$$

$$= 50 + 24(-0.577) = 36.15$$

and

$$\log n \int_0^\infty Z^4 e^{-z}\,dZ = 4! \log n = 24 \log n$$

so that

$$\mathrm{III} = \sum_1^\infty \frac{36.2 - 24 \log n}{n^5} = 36.8$$

Finally,

$$\epsilon_H = \frac{15}{\pi^4}(A_H\mathrm{I} - B_H\mathrm{II} + C_H\mathrm{III} - D_H\mathrm{IV})$$

$$= 0.766(\rho T)^{1/2} - (0.309 - 0.0889 \log \rho T)\rho T - 0.0175(\rho T)^{3/2} + \ldots \quad (41)$$

where it has been assumed that $C_2 = 1.439$.

This result which was obtained by a direct integration of the angular distribution of the spectral emissivity should be compared with the equation of Davisson and Weeks (ref. 2) which was derived by the integration of an artificially constructed function to represent the angular distribution of the spectral emissivity. They found that

$$\epsilon_H = 0.751(\rho T)^{1/2} - 0.632(\rho T) + 0.670(\rho T)^{3/2} - 0.607(\rho T)^2 \quad (42)$$

Although this equation gives values that are in good agreement with those given by equation (41) for ρT values up to 0.1, it is not useful at much larger values of ρT because it does not converge rapidly enough. Schmidt and Eckert (ref. 6), also using graphical integration, expressed their result as two binomials, for two ranges of ρT,

$$0 < \rho T < 0.2 \quad \epsilon_H = 0.751(\rho T)^{1/2} - 0.396\rho T$$

$$0.2 < \rho T < 0.5 \quad \epsilon_H = 0.698(\rho T)^{1/2} - 0.266\rho T \quad (43)$$

In treating the general case where $y \neq 0$ the total hemispherical emissivity is again given by

$$\epsilon_H=\frac{1}{\sigma T^4}\int_0^\infty \frac{\epsilon_{ph}+\epsilon_{nh}}{2} J_\lambda \, d\lambda$$

$$=\frac{15}{\pi^4}\int_0^\infty \frac{\epsilon_{nh}+\epsilon_{ph}}{2} x^3 \sum_{n=1}^{\infty} \exp(-nx)\, dx$$

and from equations (35) and (36)

$$\frac{\pi^4}{15}\epsilon_H=\sum_{n=1}^{\infty}\int_0^\infty \left\{\frac{8j}{3}\left(\frac{\rho T}{30C_2}\right)^{1/2} x^{1/2}-j^2\left(\frac{\rho T}{30C_2}\right) x \right.$$

$$\left[\frac{1}{2}+\log 60C_2-\log \rho T-\log x-\frac{1}{2}\log(1+y^2)\right.$$

$$\left.+y\pi-\frac{y}{j}\left(\frac{\rho T}{30C_2}\right)^{1/2} x^{1/2}-2y\tan^{-1} j^2\right]$$

$$\left.-\frac{3}{5}j^3\left(\frac{\rho T}{30C_2}\right)^{3/2} x^{3/2}\right\} x^3 \exp(-nx)\, dx \qquad (44)$$

where $\tan^{-1}[2(30\lambda/\rho)^{1/2}j+j^2]$ has been expanded to yield $(\pi/2)-(\rho/30\lambda)^{1/2}(1/2j)+\ldots$ by assuming in this case that $2(30\lambda/\rho)^{1/2}>>j$.

By comparing the first term of equation (44) with the first term of equation (18) it can be seen that the first term of the total hemispherical emissivity will always be 4/3 times that for the total normal emissivity regardless of the relaxation time. The other terms for the total hemispherical emissivity are calculated by a combination of graphical and analytical techniques similar to those used previously for the total normal emissivity and for the zero relaxation time case for the total hemispherical emissivity.

The results are presented here for the same five values of a as those used for the total normal emissivity.

For $a=0$,

$$\epsilon_H=0.766(\rho T)^{1/2}-(0.309-0.0889\log \rho T)\rho T$$
$$-0.0175(\rho T)^{3/2}$$

For $a=0.2$,

$$\epsilon_H=0.534(\rho T)^{1/2}-(0.218-0.0411\log \rho T)\rho T$$
$$+0.0141(\rho T)^{3/2}$$

For $a=0.5$,

$$\epsilon_H=0.384(\rho T)^{1/2}-(0.172-0.0208\log \rho T)\rho T$$
$$+0.0306(\rho T)^{3/2}$$

For $a=1.0$,

$$\epsilon_H=0.281(\rho T)^{1/2}-(0.153-0.0109\log \rho T)\rho T$$
$$+0.0461(\rho T)^{3/2}$$

For $a=1.5$,

$$\epsilon_H=0.232(\rho T)^{1/2}-(0.148-0.0076\log \rho T)\rho T$$
$$+0.0570(\rho T)^{3/2} \qquad (45)$$

These equations are plotted in figure 3.

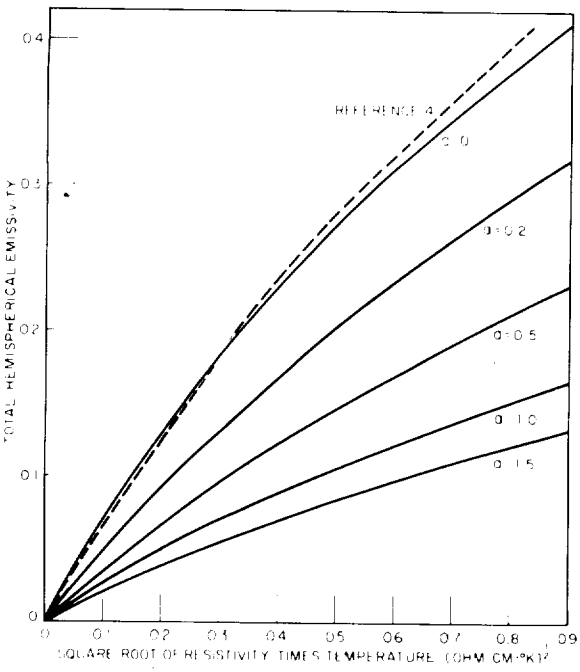

FIGURE 3.—*Total hemispherical emissivity.*

TOTAL EMITTANCE MEASUREMENTS

Radiation Measurements

The total hemispherical emittance was determined by measuring the temperature and the power dissipation in the uniform temperature region of an electrically heated ribbon specimen. Simultaneously, the angular distribution of radiation from the specimen was measured with a calibrated total-radiation thermopile, from which the total normal emittance was determined. The details of the experimental apparatus and techniques have been described previously (ref. 7 and 8).

Figure 4 is a photograph showing the ribbon support structure and other pertinent components within the vacuum chamber. The total emittances of four refractory metals

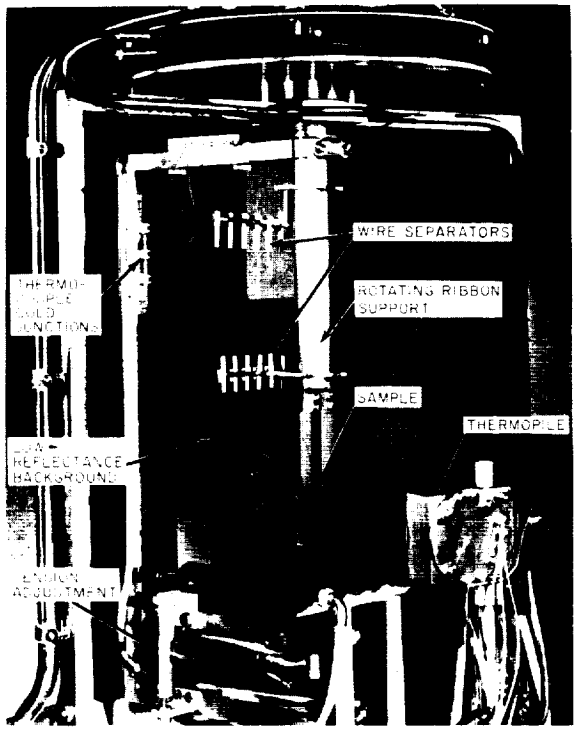

FIGURE 4.—*Experimental apparatus.*

measured with this technique are presented with a discussion of the problem of temperature determination above 2000° K.

Temperature Determination

The radiant energy emitted by a polished metal surface is proportional to about the fifth power of temperature since, in the equation $H=\epsilon_H \sigma T^4$, the total hemispherical emittance ϵ_H is roughly proportional to the temperature. Accordingly, the temperature is by far the most important variable in any radiation-transfer problem. Unfortunately, its importance is only exceeded by its difficulty of measurement, particularly in the region above 1800° K. Excellent results had been obtained with platinum thermocouples up to 1800° K in previous phases of this project; and it was hoped that refractory-metal thermocouples (tungsten/tungsten, 26-percent rhenium) would provide accurate measurements of temperatures up to 3000° K. Unfortunately, the accuracy and reproducibility were found to be far below that necessary for accurate emittance measurements.

Tungsten/tungsten, 26-percent rhenium thermocouples 0.005 inch in diameter (hereafter designated as W/Re) were obtained from two manufacturers. The first type (referred to as type A) was supplied with a calibration up to 2800° C. The second (referred to as type B) was supplied with a notary-certified calibration up to 2300° C. The type A thermocouple was tried initially on a tantalum ribbon. The wires were attached by drilling 0.005-inch holes in the center of the ribbon about 2 mm apart, inserting the wires through the holes a short distance, and then squeezing the wire by peening the ribbon around the wire with the aid of a punch with rounded nose and a center hole to accommodate the end of the wire. Excess wire was then clipped off. Measured total and spectral emittance values were found to be completely unrealistic. Similar measurements with other ribbons of the same material gave emittances that were not only unrealistic but not reproducible.

The same problem was encountered with type B thermocouples; however, in this case the emittance values at temperatures up to 2000° K appeared at least reasonable, although some nonreproducibility was still noted. Some ribbons were then instrumented with both type A and type B W/Re thermocouples, as well as with a platinum/platinum, 10-percent rhodium thermocouple. Up to 1800° K, type B agreed reasonably well with the platinum thermocouple, whereas type A deviated considerably. Emittances calculated from the platinum-measured temperatures were quite within expectation.

It was evident that a complete calibration of the W/Re thermocouples was necessary before they could be used. A tantalum cylinder ¾ inch in diameter and ½ inch deep was instrumented with type A and type B W/Re thermocouples. Two platinum/platinum, 10-percent rhodium thermocouples, one a 0.005-inch working thermocouple and the other a 0.008-inch calibrated standard, were also used. Blackbody holes 0.016 inch in diameter were drilled at various places in the surface. The assembly was placed in the coil of an induction heater and heated in vacuum up to 1800° K. A microoptical pyrometer was used to monitor

the temperature in the blackbody holes. Temperature readings of the pyrometer, the two platinum thermocouples, and the type B W/Re thermocouple agreed well within ±1 percent over this range, whereas type A deviated as much as 80° C. The platinum thermocouples were then removed, and the comparison was extended to the highest temperature obtainable in the furnace, 2100° K. Type B and the pyrometer remained in agreement to within ±1 percent whereas type A continued to show large deviations. Although the temperature limit was far below the 3000° K desired, and the thermocouples were not tested in their normal mode of operation (attached to the ribbon), this calibration at least eliminated one of the theremocouples from further consideration.

In order to calibrate the thermocouples in their normal mode of operation, it was necessary to determine the spectral emittance of tantalum as an intermediate step. A tantalum ribbon, 1 cm wide, 6 inches long, and 0.005 inch thick, was folded longitudinally to form a triangular prism with sides approximately ⅓ cm wide. The length of the prism was about 4 inches. Several 0.005-inch and 0.010-inch holes were drilled into one side to serve as blackbody holes. The prism was instrumented with type B W/Re thermocouples and aged at 2400° K for 15 minutes.

Measurements of true temperature, brightness temperature of the tantalum surface, and thermocouple output voltage were made from 1000° K to 2800° K. The true temperature was obtained by sighting the optical pyrometer at the blackbody holes; the brightness temperature of the surface was taken adiacent to the holes. The resulting spectral emittance at 0.65 micron is plotted in figure 5. The upper temperature limit was set by the evaporation of the tantalum above 2800° K, which produced sufficient coating on the viewing port to prevent further optical pyrometer observation. A calibration was also obtained for the attached thermocouples, although another check was still necessary for the thermocouples in their normal mode of operation (on a flat strip).

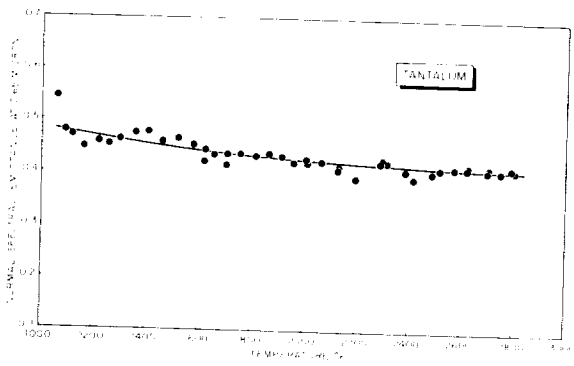

FIGURE 5.—*Spectral emittance of tantalum at 0.65μ.*

As an added complication, two identical microoptical pyrometers, one recently acquired, the other on hand for 2 years or more, were compared and found to differ by as much as 1 percent in their indicated temperatures. The error was largest in the range of 1800° C to 2200° C. Below this temperature they were nearly identical in calibration. Above this range there was an error but not as serious. These pyrometers have now been recalibrated at the Naval Ordnance Laboratory at Corona, Calif.

Another 6-inch section of the ribbon identical to that which had been formed into the prism was instrumented and aged as before; however, this time the section was used as a flat ribbon. Brightness-temperature measurements, and the calibration data of figure 5 were used to obtain the true temperature, and the thermocouple was again calibrated, with results nearly identical to those of the previous measurement. Hence, a calibration was obtained for type B W/Re thermocouples from 1000° K to 2800° K in their normal mode of operation. The previously mentioned nonreproducibility of emittance data was essentially eliminated by adopting one thermocouple attachment technique, out of the many tried, that gave reproducible results. This technique consisted of inserting the thermocouple wire through the hole in the ribbon, then spreading the end of the wire slightly, and pulling the wire vigorously back into the hole. The wedging was sufficient to hold the wire, and the attachment eliminated the ribbon deformation caused by peening. Results of many measurements confirm the reproducibility of this method. The calibration was within ±1 percent of

that supplied with type B thermocouples up to 2150° K. Above this temperature the deviation increased rapidly; it was 90° at 2600° K. In the following description of results, the over-all temperature accuracy is estimated to be within ±1 percent to 2800° K and ±1.5 percent from 2800° K to 3000° K. A calibration for the range from 2800° K to 3000° K was obtained by various means of extrapolation. Measurements on tungsten, described in the following section, added confidence to this extrapolation.

Results

TANTALUM

The total hemispherical emittance and the total normal emittance of tantalum, plotted against temperature, are presented in figure 6. The data points for the hemispherical emittance represent measurements from four different samples using both brightness temperature and thermocouple data to determine emittance. At low temperatures tantalum exhibits a gettering action for gases in the vacuum system, with a corresponding increase in the hemispherical emittance, shown by the short dashed line between 1200° K and 1500° K. If the emittance is measured on a fresh unaged tantalum ribbon, it will follow the dashed line to about 1500° K where the gases will be driven off resulting in a sudden drop in the emittance to the solid line. Measurements above this temperature appear quite stable. If, after aging, measurements are made below 1500° K with dispatch, the data will fall on the solid line. However, if a temperature below 1500° K is maintained for an extended period the emittance returns to the dashed line (rate depends on pressure). The gas absorption and liberation can be noted on the vacuum gage connected to the measuring chamber. A separate study of emittances would be advised for those interested in long-term heat-transfer properties below 1500° K.

The total normal emittance shown in figure 6 is calculated from the ratio of total hemispherical to total normal emittance determined from relative angular distribution measurements every 300° K from 1200° K to 2400° K. At the time that angular distribution measurements were being made on tantalum, the thermocouple had not yet had an absolute calibration check so that no total normal emittance values were determined based on absolute normal radiation. The spectral emittance at 0.65 micron is determined with the aid of true and brightness temperatures acquired during the prism thermocouple calibration and plotted against temperature in figure 5.

NIOBIUM

A gettering action similar to that observed with tantalum is exhibited by niobium except that the transition, or outgassing, temperature appears to be 1400° K. This effect can be seen in figure 7, which shows total hemispherical emittance and total normal emittance plotted against temperature up to 2400° K. Evaporation prevented measurements above this tem-

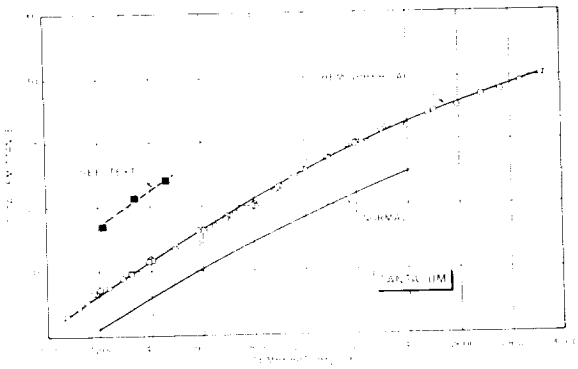

FIGURE 6.—*Total emittance of tantalum.*

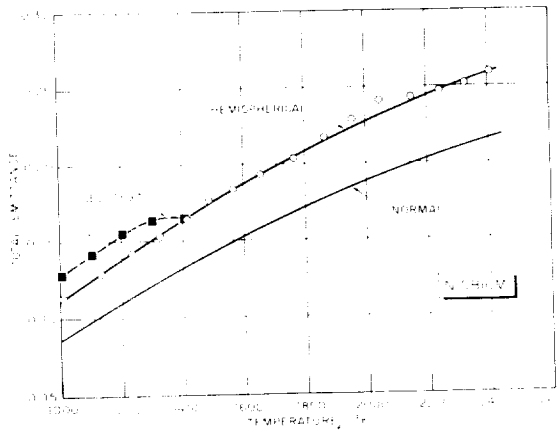

FIGURE 7.—*Total emittance of niobium.*

perature. The total normal emittance was determined from calibrated thermopile measurements. True temperatures for the niobium measurements were determined with the thermocouples calibrated as previously described.

TUNGSTEN

Considerable effort has been expended by other investigators in studying the thermal-radiation properties of tungsten, with much of the impetus coming from its use by the lighting industry. Consequently, the relation between brightness and true temperature, as determined by Roeser and Wensel and shown in the survey by Gubareff et al. (ref. 9), has been used to obtain the true temperature in this research. Concurrently, however, the calibrated type B W/Re thermocouple was also used.

The total hemispherical emittance, which is quite sensitive to temperature differences, has about ±5-percent spread with both temperature-measuring techniques, as can be seen in figure 8. The emittance determined with the brightness temperature (data points indicated by circles) appears generally to be a few percent higher in the middle and upper temperature regions. Considering the problems associated with the thermocouples at high temperatures, and the possible nonequivalence of the tungsten surface used in this investigation and that of Roeser and Wensel, this difference is not surprising. The uncertainty in optical-pyrometer temperatures in the vicinity of 2100° K, pointed out in the section on temperature determination, could contribute to the wider spread in this region. The reasonable agreement of the results obtained by the two techniques was the basis for using brightness-temperature data to help extrapolate the thermocouple calibration from 2800° K to 3000° K. The tungsten samples used were aged at 2400° K for approximately 30 minutes. The total normal emittance shown in figure 8 was determined with the calibrated thermopile.

MOLYBDENUM

The measurements on molybdenum preceded those on the other metals just discussed, and were made in an earlier apparatus which was originally used for studies of platinum (ref. 10). At first a very high emittance was observed. Although it was quite stable, it was later determined to be due to the formation of molybdenum carbide, Mo_2C, possibly caused by backstreaming of the vapor from the oil diffusion pump. The coating still formed at 10^{-6} torr, but at that pressure it was possible to obtain meaningful emittance measurements provided that they were made rapidly enough.

Figure 9 illustrates the change in emittance with time as well as temperature on a typical specimen. The average time between measurements was about 1 minute. By the time of the fifth measurement there was apparently some increase in emittance due to the coating. After 10 minutes at 1300° K the emittance reached the nearly stable upper curve of emittance versus temperature. The points 1, 2, 3, and 4 are characteristic of the emittance of a polished

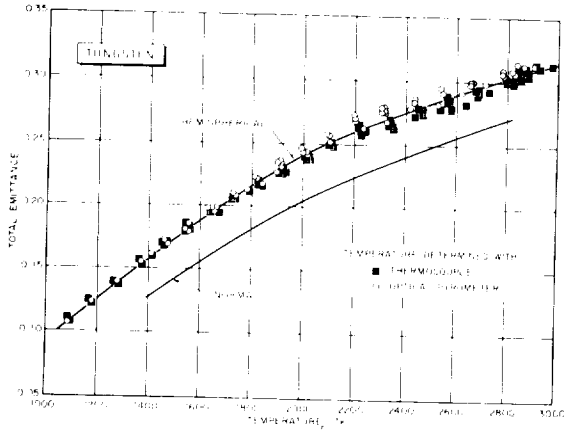

FIGURE 8.—*Total emittance of tungsten.*

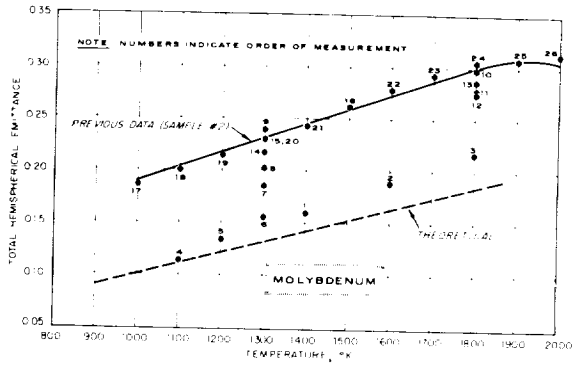

FIGURE 9.—*Total emittance of molybdenum.*

surface. The points 9 through 26 establish the emittance of a surface with a nearly stabilized coating of molybdenum carbide. The difficulty arising from this coating was one of the reasons for designing the new emittance chamber which was used for the other three metals (ref. 11). The overall accuracy of the total-emittance values quoted for the four metals is ± 5 percent.

ELECTRICAL RESISTIVITY

Because of the importance of the electrical resistivity in the theory of emissivity, the variation of this property with temperature was

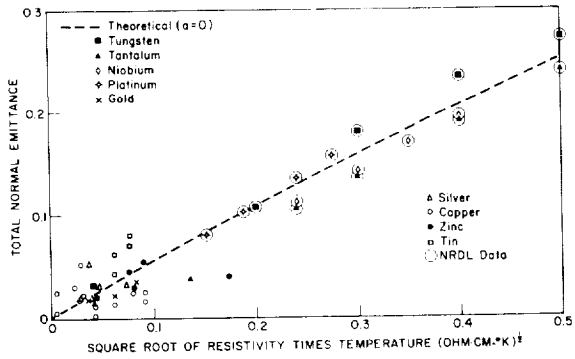

FIGURE 10.—*Total normal emittance of various metals.*

measured (ref. 7 and 11) for all four metals over the complete temperature range of the emittance measurements. These values were used to determine the abscissas in figures 10 and 11.

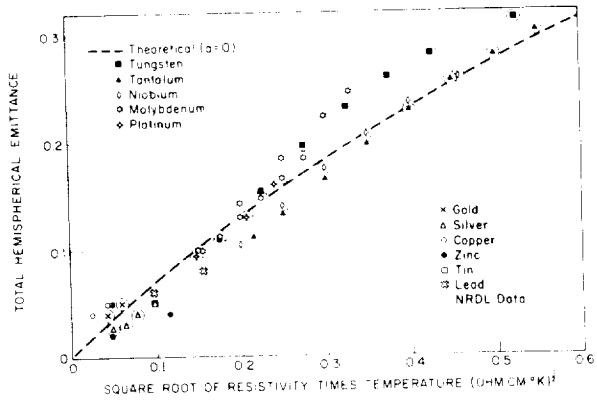

FIGURE 11.—*Total hemispherical emittance of various metals.*

SPECTRAL EMITTANCE MEASUREMENTS

The previously described experimental apparatus has been modified slightly to facilitate spectral emittance measurements on the refractory metals. The specimen configuration is a long triangular tube formed by clamping three ribbons together at the ends to form a 60° triangular prism. In order to insure that the three edges of the prism remain closed, it is wrapped with fine tungsten wire. A small 1×3 mm rectangular hole in one face of the prism serves as the reference blackbody. A Perkin-Elmer double-pass infrared spectrometer is used, and the external optics allow the blackbody hole and the face of the sample adjacent to the hole to be focused alternately on the entrance slit of the spectrometer. In this way a direct comparison may be made of the radiation from the metallic surface with that of a blackbody at the same temperature. The technique is similar to that used by De Vos in his determination of the normal spectral emittance of tungsten between 0.25 and 2.5 microns (ref. 3).

At present the measurements are being made between 0.6 and 5.00 microns; the long-wavelength limit is determined by the sapphire window in the vacuum chamber and the lithium fluoride prism in the spectrometer, and the short-wavelength limit is determined by the low energy available there. A photomultiplier is used as the detector from the visible to 1 micron, and a thermocouple is used as the detector beyond 1 micron. The present studies are of normal spectral emittance only; however, the angular rotation capabilities of the ribbon mount permit hemispherical spectral emittance measurements to be made. These will be included in future studies in which the wavelength range will be extended to 25 microns and the angular distribution will be determined for each plane of polarization. Since the prism is instrumented with thermocouples and voltage probes, the total hemispherical emittance can be obtained both from the power measurement and from the integral of the spectral emittance over the significant wavelength region and over all angles in both planes of polarization.

Tungsten has been used for the initial study, in order that comparison of the results with the reliable data of De Vos (ref. 3) might provide an evaluation of the performance of the system. Agreement has been within a few percent in the region from 0.6 to 2.5 microns.

DISCUSSION OF DATA

The total normal and total hemispherical emittance data obtained on this project are plotted against the square root of the electrical resistivity multiplied by the absolute temperature in figures 10 and 11. Data from the recent thermal radiation survey of Gubareff et al. (ref. 9) are also included; these data were reported for polished surfaces with no additional characterization. The interesting features are the wide spread of data points, particularly at low values of ρT, and the qualitative agreement with the theoretical (dashed) curves through an extended range of ρT. These curves are taken from figures 2 and 3 for the $a=0$ case. In figure 10 the dashed curve provides about as good a fit as possible for the plotted data. This may seem surprising since it has been shown previously in this article that the finite relaxation time should reduce the total emissivity of all the metals by about 30 to 70 percent as indicated in figures 2 and 3. However, there are some compensating factors which serve to increase the emissivity. The resistivity at the surface will be higher than in the interior due to scattering of the electrons by the interface and by imperfections in the lattice induced by surface preparation. The absicissa in figures 10 and 11 is calculated from the bulk resistivity. The emissivity depends upon an effective value of the resistivity within the penetration depth of the electromagnetic wave, which is of the order of 1000 Å at the peak of the spectral distribution. At very low temperatures the mean free path of the electron may be greater than the penetration depth and the effective resistivity becomes very much higher. This phenomenon is referred to as the anomalous skin effect (ref. 12).

It is only the transition metals which have high values of ρT; the high values are due to their high melting points and relatively large electrical resistivities. Both of these characteristics depend upon the fact that electrons are both in the incompletely filled d shells of these atoms and in the s shells in the next higher energy level. The transfer of electrons between these shells gives rise to the absorption and emission of radiation in the near infrared and can contribute to the spectral emissivity at short wavelengths and thus to the total emissivity at high temperatures.

The equations developed in this report ignore the effect of the bound electrons which become important at short wavelengths where the effect of the free electrons becomes much less pronounced. Corrections need to be applied to the total emissivity at high temperatures in order to take these electrons properly into account.

Some work has been done elsewhere (ref. 13) in trying to correlate theory and experiment by assuming the existence of different relaxation times for various groups of free electrons in the same metals.

As for the spread of data, which is particularly severe at low values of $(\rho T)^{1/2}$, this is due to several general causes. The extent of the corrections just discussed is different for each metal. The specimens measured may not have been ideal in the sense of complete freedom from thin surface films, imperfections behind the surface, or surface roughness. Emittance measurements are difficult to make and experimental errors can be quite large. Very accurate temperature determinations are required unless the blackbody reference standard is automatically at the same temperature as the specimen. Small percentage errors in reflectance can result in large percentage errors in emittance if the indirect reflectance measurement technique is used.

REFERENCES

1. Foote, P. D.: Bull. Nat. Bur. Stand. 11, 607 (1914–1915).
2. Davisson, C., and Weeks, J. R., Jr.: The Relation Between the Total Thermal Emissive Power of a Metal and Its Electrical Resistivity. Jour. Optical Soc. of America, vol. 8, no. 5, May 1924, pp. 581–605.
3. De Vos, J. C.: A New Determination of the Emissivity of Tungsten Ribbon. Physica, vol. 20, no. 10, Oct. 1954, pp. 690–714.
4. Stratton, Julius Adams: Electromagnetic Theory. McGraw-Hill Book Co., Inc., 1941, p. 496.

5. MOTT, N. F., and JONES, H.: The Theory of the Properties of Metals and Alloys. Oxford Univ. Press, 1936, p. 112.
6. SCHMIDT, E., and ECKERT, E.: Directional Distribution of Heat Radiation From Surfaces. Forschung. Geb. Ing.-Wes., vol. 6, July–Aug. 1935, pp. 175–183.
7. ABBOTT, G. L.: Total Normal and Total Hemispherical Emittance of Polished Metals, Part III. WADD Tech. Rep. 61–94, U.S. Air Force, Sept. 1963.
8. ABBOTT, G. L.: Total Normal and Total Hemispherical Emittance of Polished Metals. Measurement of Thermal Radiation Properties of Solids, Joseph C. Richmond, ed., NASA SP–31, 1963, pp. 293–306.
9. GUBAREFF, G. G., JANSSEN, J. E., and TORBORG, R. H.: Thermal Radiation Properties Survey. Second ed., Honeywell Res. Center, Minneapolis-Honeywell Regulator Co., 1960.
10. ABBOTT, G. L., ALVARES, N. J., and PARKER, W. J.: Total Normal and Total Hemispherical Emittance of Polished Metals, Part I. WADD Tech. Rep. 61–94, U.S. Air Force, Nov. 1961
11. ABBOTT, G. L., ALVARES, N. J., and PARKER, W. J.: Total Normal and Total Hemispherical Emittance of Polished Metals, Part II. WADD Tech. Rep. 61–94, U.S. Air Force, Jan. 1963.
12. REUTER, G. E. H., and SONDHEIMER, E. H.: The Theory of the Anomalous Skin Effect in Metals. Proc. Roy. Soc. (London), ser. A., vol. 195, no. 1042, Dec. 22, 1948, pp. 336–364.
13. ROBERTS, S.: Optical Properties of Nickel and Tungsten and Their Interpretation According to Drude's Formula. Phys. Rev., ser. 2, vol. 114, no. 1, Apr. 1, 1959, pp. 104–115.

DISCUSSION

H. E. BENNETT, Michelson Laboratory, U.S. Naval Ordnance Test Station: I would like to make one comment that may give some hope for the theoretical calculation. The Hagen-Rubens relation is derived by assuming that n and k are equal, which is true only for very long wavelengths. With decreasing wavelength the Hagen-Rubens relation gives higher emittance values, or lower reflectance values, than are obtained by using the exact theory. However, if surface damage is present, the measured emittance *is* higher, and the measured reflectance *is* lower than would be true for an undamaged sample. Therefore, although the Hagen-Rubens relation does not have a good theoretical justification in short-wavelength regions, it frequently fits the experimental data better than does the exact theory.

PARKER: Surface damage is certainly one of the things that should be considered. Several additional factors are involved in this wavelength range, but all of them seem to average out and the data approximately follow the curve based on the assumption that the relaxation time is equal to zero.